0026-895X/00/010037-11$3.00/0
MOLECULAR PHARMACOLOGY

MOL 58:37–47, 2000 /13011/828850

Functional Analysis of a Tryptophan-Less P-glycoprotein: A Tool for Tryptophan Insertion and Fluorescence Spectroscopy

TONY KWAN, HELEN LOUGHREY, MARTINE BRAULT, SAMANTHA GRUENHEID, INA L. URBATSCH, ALAN E. SENIOR, and PHILIPPE GROS

Department of Biochemistry, McGill University, Montreal, Quebec, Canada (T.K., M.B., S.G., P.G.); Department of Biochemistry, National University of Ireland, Galway, Ireland (H.L.); and Department of Biochemistry and Biophysics, University of Rochester Medical Center, Rochester, New York (I.L.U., A.E.S.)

Received October 4, 1999; accepted March 7, 2000

This paper is available online at http://www.molpharm.org

ABSTRACT

P-glycoprotein (Pgp) functions as an ATP-dependent drug efflux pump to confer multidrug resistance to tumor cells. In the absence of a high-resolution structure for this protein, several important and intriguing aspects of Pgp structure and function remain poorly understood. Fluorescence spectroscopy of endogenous or genetically engineered tryptophan residues represents a potentially powerful method to probe static and dynamic aspects of Pgp at high resolution. We have used site-directed mutagenesis to modify the wild-type (WT) mouse *mdr3* Pgp for tryptophan fluorescence spectroscopy by replacement of all 11 tryptophan residues individually with phenylalanine. None of the 11 tryptophans were found to be absolutely essential for Pgp activity, because Chinese hamster ovary cells transfected and overexpressing this mutant Trp-less mdr3 cDNA (*mdr3*F_{1-11}) become multidrug-resistant and can carry out active transport of vinblastine, colchicine, and Calcein-AM. The *mdr3*F_{1-11} mutant has reduced activity compared with WT Mdr3, and shows a unique pattern of drug resistance clearly distinct from WT and, as opposed to the latter, can neither confer FK-506 resistance nor functionally complement *ste6* in yeast. Studies with Pgp mutants containing either single or double tryptophan residues or with chimeric molecules constructed between wild-type Pgp and *mdr3*F_{1-11} indicated that no single tryptophan residue was responsible for the reduced activity of the *mdr3*F_{1-11} mutant. Likewise, all but one chimeric Pgp preserved the unique drug resistance profile of the *mdr3*F_{1-11} mutant. Altogether, we show that a Trp-less Pgp is functionally active and can be used as a molecular backbone for insertion of tryptophans in strategic locations to probe various aspects of Pgp function.

Multidrug resistance (MDR) in certain tumors in vivo and in cultured cell lines in vitro is phenotypically defined by cross-resistance to structurally and functionally dissimilar compounds. In many cases, MDR is associated with overexpression of members of the P-glycoprotein (Pgp) family (Hanna and Gros, 1996). These are integral membrane proteins that function as energy-dependent efflux pumps to reduce intracellular drug accumulation. Pgps are encoded by a small family of two closely related genes in humans (*MDR1* and *MDR2*) and three genes in mouse (*mdr1*, *mdr2*, and *mdr3*). In normal tissues, Pgps function as lipid flippases (Ruetz and Gros, 1994) to translocate different types of phospholipids from the inner to outer leaflets of the lipid bilayer in the canalicular membrane of hepatocytes (Schinkel et al., 1994) and possibly in other membranes as well (Vanhelvoort et al., 1996). The mechanism of drug transport by Pgps may be similar to the translocase mechanism of lipid transport demonstrated in normal tissues (Ruetz and Gros, 1994). Pgps belong to the superfamily of ATP-binding cassette transporters, which has been conserved in eukaryotes and prokaryotes (Ling, 1997). Structural homology among ATP-binding cassette transporters translates into functional similarity, as Pgp (Mdr3) (Raymond et al., 1992) can functionally complement null mutations at the yeast *ste6* homolog.

Hydropathy profiling (Gros et al., 1986), accessibility to protease cleavage sites (Yoshimura et al., 1989), epitope mapping of inserted antigenic peptides (Kast et al., 1996), photoaffinity labeling (Greenberger, 1993), and modification by sulfhydryl reagents (Loo and Clarke, 1995b) have been used to identify structural features of Pgp, and to establish structure/function relationships. Pgp is organized into two symmetrical halves, each consisting of six transmembrane (TM) domains and one nucleotide binding (NB) site. Indepen-

This work was supported in part by a grant (to P.G.) from the Medical Research Council (MRC) of Canada and by National Institutes of Health Grant GM50516 (to A.E.S.). T.K. was supported by a studentship from la Formation de Chercheurs et l'Aide à la Recherche, and P.G. was supported by a senior Scientist Award from the MRC.

ABBREVIATIONS: MDR, multidrug resistance; Pgp, P-glycoprotein; TM, transmembrane; NB, nucleotide binding; CHO, Chinese hamster overy; MEM, minimal essential medium; VBL, vinblastine; ADM, Adriamycin; PAGE, polyacrylamide gel electrophoresis; COL, colchicine; ACT, actinomycin-D; VRP, verapamil; VBL^R, VBL-resistant; $G418^R$, G418-resistant.

dent lines of investigation have suggested that the TM domains are the primary sites of protein-substrate interaction. These studies include epitope mapping studies of tryptic peptides labeled with drug analogs (Greenberger, 1993) as well as the altered drug-resistance profiles encoded by Pgps bearing naturally occurring (Devine et al., 1992) or experimentally induced mutations in TM domains (Loo and Clarke, 1994; Hanna et al., 1996; Hafkemeyer et al., 1998). Pgp has two NB sites of the Walker type that have been positioned intracellularly (Kartner et al., 1985; Yoshimura et al., 1989). Biochemical studies of purified wild-type protein (Senior, 1998; Shapiro and Ling, 1998) and genetic studies with site-directed mutants in the Walker A and B motifs (Azzaria et al., 1989) have shown that ATP binding and hydrolysis at both NB sites are required for Pgp function. Complete cooperativity is required between the two NB sites because mutations at one site abrogate ATP hydrolysis by the protein (Urbatsch et al., 1998). An alternate site catalysis model has been proposed as a mechanism for ATP hydrolysis by Pgp (Senior, 1998). A unique property of its ATPase activity is that it can be strongly stimulated by either substrates or inhibitors of Pgp transport (Senior, 1998; Shapiro and Ling, 1998).

Although significant progress has been made identifying regions of Pgp involved in drug binding and ATP hydrolysis, important structural and functional aspects of Pgp remain poorly understood. These include identifying the structural determinants responsible for the 1) broad substrate specificity of Pgp, 2) signaling between TM domains and NB sites to mediate activation of ATPase activity and drug efflux, and 3) cooperativity between the two NB sites for ATP hydrolysis. A high-resolution structure of Pgp together with dynamic information will ultimately be needed to answer these questions accurately. In the absence of more detailed structural information, other methods based on site-specific modification with sulfhydryl reagents in single cysteine mutants have been used to monitor changes in the local environment of specific residues and to establish structure/function relationships (Liu and Sharom, 1996; Loo and Clarke, 1997b). Fluorescence spectroscopy of endogenous tryptophan residues represents a powerful alternative method for probing static and dynamic aspects of Pgp at high resolution (Wang et al., 1997; Weber et al., 1998). One major problem is the complexity of the signal that results from the presence of multiple tryptophan residues, 11 in Pgp. This restricts the ability to monitor environmental changes of a specific natural or experimentally introduced tryptophan, which could be associated with discrete stages of substrate binding, transport, or enzymatic activity. Alternatively, naturally occurring tryptophans can be removed to create a tryptophan minus (Trp-less) backbone onto which individual tryptophans can be reintroduced at strategic positions of the protein.

For this reason, we have initiated studies on Pgp using site-directed mutagenesis to determine which tryptophan residues can be replaced by phenylalanine without loss of function. We found that a Pgp mutant completely devoid of tryptophans retains sufficient activity to confer drug resistance in transfected mammalian cells and can hydrolyze ATP once purified and reconstituted. Finally, we have constructed single and double tryptophan Pgp mutants that retain very robust activity and that, together with the Trp-less molecule, provide suitable backbones for site-directed tryptophan replacements and analysis by fluorescence spectroscopy.

Materials and Methods

Site-Directed Mutagenesis and Plasmid Construction. To create a Pgp mutant lacking tryptophan residues (F_{1-11}), the amino-terminal (1.7-kb *Sph*I from polylinker, to *Sma*I, position 1767) and the carboxyl-terminal (1.7-kb *Sma*I, position 1767, to *Pst*I, position 3516) half of a mouse *mdr3* cDNA cloned in pGEM7Zf were introduced in the corresponding restriction enzyme sites of plasmid vector M13 mp19, as described previously (Kast et al., 1995; Hanna et al., 1996). The W44F (F_1), W132F (F_2), W158F (F_3), W208F (F_4), W228F (F_5), and W311F (F_6) mutations were introduced sequentially on the *mdr3* amino-terminal template to generate the *mdr3*F_{1-6} mutant in which the 6 Trp residues from the amino-terminal half of Mdr3 are replaced by the structurally similar Phe. In parallel, the W694F (F_7), W704F (F_8), W809F (F_9), W851F (F_{10}), and W1104F (F_{11}) mutations were introduced in the carboxyl-terminal template to generate the *mdr3*F_{7-11} mutant. The two mutated *mdr3* halves were then reassembled into a full-length *mdr3* cDNA encoding a Pgp mutant devoid of tryptophan residues (Mdr3F_{1-11}) as follows: the *Afl*II (position 169) to *Sma*I (position 1767) fragment of M13*mdr3*F_{1-6} was first inserted into the corresponding sites of plasmid pGEM7Zf, followed by insertion of the *Sma*I (position 1767) to *Pst*I (position 3516) fragment from M13*mdr3*F_{7-11} to create pGEM*mdr3*F_{1-11}. Briefly, site-directed mutagenesis was carried out on single stranded DNA template using a commercially available in vitro system (Sculptor system, Amersham Pharmacia Biotech) and mutagenic oligonucleotide primers listed in Table 1. The presence of specific site-directed mutations and the integrity of the rest of the sequence of the *mdr3* cDNA inserts used were verified by nucleotide sequencing, before reassembling of the full-length *mdr3*F_{1-11} mutant. For expression in Chinese hamster ovary (CHO) (LR73) cells, the *mdr3*F_{1-11} cDNA from pGEM*mdr3*F_{1-11} was excised as a 4.1-kb *Kpn*I/*Cla*I fragment (polylinker sites) and reinserted into the corresponding sites of mam-

TABLE 1
Oligonucleotides used for site-directed mutagenesis of mouse *mdr3*
All oligonucleotides are in the antisense orientation. Underlined codons are mutant positions.

Amino Acid Mutant (W → F)	Primer Sequence	5′ Nucleotide
W44F (F_1)	5′-CCTGTCCAGGAAACCTGCATAAC-3′	292
W132F (F_2)	5′-CTGCCAGGCAGAAAAATGAAACC-3′	557
W158F (F_3)	5′-CACATCAAAGAAGCCTATCTC-3′	634
W208F (F_4)	5′-GGTTAGCTTGAAGCCACGGGT-3′	784
W228F (F_5)	5′-CAATATCTTTGCGAAAATACCAGC-3′	847
W311F (F_6)	5′-GAAGTCCCATAGAAGAATGCCAACGCGTATGATGCATAG-3′	1095[a]
W694F (F_7) and W704F (F_8)	5′-CAAAATAAGGGAATTCAGTTGAATTCAACTTCAGGATCCGGAAAAAGGAAGC-3′	2273
W799F (F_9)	5′-GTCATCAAAGAAGCTCACATC-3′	2557
W851F (F_{10})	5′-GTGTTAGTTGGAAGCCATAGA-3′	2714
W1104F (F_{11})	5′-GTGCTCGGAGGAACTGGACATTC-3′	3473

[a] Additional introduction of the *Mlu*I site.

malian expression vector pCB6 (Brewer, 1994). This vector contains both a *neo* cassette (G418 resistance) for drug selection in transfected cells, as well as a promoter/enhancer region of cytomegalovirus that directs high level transcription of cloned cDNA inserts. For expression in the yeast *Saccharomyces cerevisiae* and also for further subcloning of various chimeras into pCB6, the *mdr3*$F_{1–11}$ cDNA from pGEM*mdr3*$F_{1–11}$ was excised as a 3.3-kb *Afl*II (position 169) to *Pst*I (position 3516) fragment and inserted into *Afl*II/*Pst*I-digested pVT-*mdr3.5* (Urbatsch et al., 1998). The pVT plasmid contains a *ura3* marker for selection in *S. cerevisiae* and uses the alcohol dehydrogenase gene promoter to direct high level expression of inserted cDNAs (Vernet et al., 1987).

Additional mutants were constructed in which tryptophan residues were re-introduced on the backbone of the tryptophan-less *mdr3*$F_{1–11}$ mutant. For this, chimeric molecules consisting of wild-type *mdr3* and *mdr3*$F_{1–11}$ were constructed. Mutants *mdr3*$F_{1–4}$, *mdr3*$F_{5–7}$, *mdr3*$F_{5–9}$, and *mdr3*$F_{10–11}$ were created by inserting segments of pVT*mdr3*$F_{1–11}$ into the corresponding sites of pVT*mdr3*:*mdr3*$F_{1–4}$ (625-bp *Afl*II/*Msc* I fragment, positions 169–794), *mdr3*$F_{5–7}$ (1454-bp *Msc* I/*Eco*RI fragment, positions 794-2248), and *mdr3*$F_{10–11}$ (880-bp *Sal*I/*Pst*I fragment, positions 2630–3510). Mutant *mdr3*$F_{1–3}$, was created by recombinant polymerase chain reaction from two overlapping *mdr3* products: the first product was generated from plasmid template pGEM*mdr3*$F_{1–11}$ using oligonucleotide primers T7 universal (plasmid vector and EC2R, 5′-GGTTAGCTTCCAGCCGCGGGTAAATC-3′; positions 759–784), whereas the second was obtained from pVT*mdr3* as template with primer pairs EC2F, 5′-GATTTACCCGCGGCTGGAAG-3′ (positions 759–778), and CK1, 5′-GAGTATTCTCGCGAGATGACC-3′ (positions 1099–1119). The 800-bp T7/EC2R and 360-bp EC2F/CK1 products were gel-purified, mixed, denatured, and reamplified using CK1 and T7 universal primer pair. The 1.1-kb fragment product was digested with *Afl*II (position 169) and *Msc* I (position 794) and reintroduced into the corresponding sites of pVT*mdr3* to create pVT*mdr3*$F_{1–3}$. The 625-bp *Afl*II/*Msc* I fragment was also reinserted into pVT*mdr3*$F_{1–11}$ to create the single tryptophan mutant, pVT*mdr3*W208. The single tryptophan mutant pVT*mdr3*W851 and the double mutant pVT*mdr3*W208/W851 were created by introducing a 755-bp *Sal*I/*Xho*I (positions 2630–3385) fragment from pVT*mdr3* into the corresponding sites of pVT*mdr3*$F_{1–11}$ and pVT*mdr3*W208, respectively. These chimeric and mutant cDNAs in pVT were then introduced as 3215-bp *Afl*II/*Xho*I (positions 170-3385) fragments into the corresponding sites of either pCB6*mdr3* (for pVT*mdr3*$F_{1–3}$, pVT*mdr3*$F_{1–4}$, and pVT*mdr3*$F_{5–7}$) or of pCB6*mdr3*$F_{1–11}$ (for pVT*mdr3*W208, pVT*mdr3*W851, pVT*mdr3*W208/W851, and pVT*mdr3*$F_{10–11}$).

Cell Culture. Drug-sensitive LR73 CHO cells were grown in minimal essential medium (α-MEM) supplemented with 10% fetal calf serum, 2 mM L-glutamine, and penicillin (50 U/ml) and streptomycin (50 μg/ml). pCB6*mdr3* constructs were introduced by transfection into LR73 cells as calcium chloride precipitates, as described previously (Kast et al., 1996). After 2 days, cells were subcultured (1:3 dilution), and stable transfectants were selected in medium containing G418 (1 mg/ml). Mass populations of G418-resistant ($G418^R$) transfectants were harvested after 9 days of selection and subcultured in medium containing vinblastine (VBL 25, 50, and 100 ng/ml final concentration) to obtain mass populations of drug-resistant cell clones overexpressing the Mdr3 proteins. VBL-resistant (VBL^R) populations were harvested 2 to 3 weeks later, expanded in culture, and frozen at −80°C in 90% serum and 10% dimethyl sulfoxide. In some experiments, individual VBL^R clones were picked, expanded in culture, and stored frozen until subsequent functional characterization.

Membrane Preparation and Western Blotting. Crude membrane fractions from transfected CHO cells were isolated as described previously (Kast et al., 1995). Briefly, cells were grown to 70% confluency and harvested in cold PBS containing sodium citrate. The cell pellet was homogenized (Dounce homogenizer, 50 strokes) in buffer containing 1 mM $MgCl_2$ and 10 mM Tris, pH 7.0, supplemented with protease inhibitors leupeptin (1 μg/ml), pepstatin A (1 μg/ml), aprotinin (1 μg/ml), and phenylmethylsulfonyl fluoride (1 mM). Unbroken cells and nuclei were removed by centrifugation (2000*g*, 5 min, 4°C), and a crude membrane fraction was further isolated by centrifugation of the supernatant (200,000*g*, 30 min, 4°C). The protein concentration in the crude membrane fraction was determined by the method of Bradford, using a commercially available reagent (Bio-Rad). For immunodetection of Mdr3, 10 μg of protein was resolved on an SDS-7.5% polyacrylamide gel and transferred onto a nitrocellulose membrane by electroblotting. The blots were blocked overnight at 4°C in a solution containing 1% BSA (Fraction V, fatty acid free) in TBST buffer (10 mM Tris, pH 8.0; 150 mM NaCl, 0.05% Tween 20). This was followed by incubation for 1 h with either 1 μg/ml mouse anti-Pgp monoclonal antibody C219 (Centocor Corp., Philadelphia, PA), a 1:400 dilution of mouse anti-hamster P-gp monoclonal antibody Ab-2 (NeoMarkers, Union City, CA), or a 1:200 dilution of polyclonal isoform-specific rabbit anti-mouse Mdr3 polyclonal antibodies B2037 or K2037 (Devault and Gros, 1990). Both antisera are raised against the same Mdr3-specific oligopeptide immunogen but coupled to BSA (B2037) or keyhole limpet hemocyanin (K2037). Specific immune complexes were detected using either a second goat anti-mouse antibody (1:10,000 dilution) or anti-rabbit antibody (1:10,000 dilution) coupled to peroxidase and revealed by enhanced chemiluminescence (NEN Life Science Products).

Cell Cytotoxicity Assay in Mammalian Cells. Drug cytotoxicity assays were performed using sulforhodamine B to stain cellular proteins, as described previously (Tang-Wai et al., 1993). Briefly, 7.5×10^3 cells from either VBL^R mass populations expressing individual Mdr3 proteins and drug-sensitive control LR73 cells were seeded in 96-well titer plates containing α-MEM supplemented with increasing concentrations of cytotoxic drugs VBL, colchicine (COL), actinomycin-D (ACT), and Adriamycin (ADM). The cells were incubated at 37°C for 96 h and fixed for 1 h in 17% trichloroacetic acid in PBS, and cellular protein was stained for 10 min at room temperature with 0.4% sulforhodamine B in 1% acetic acid. The plates were washed with water and dried, and the stain was dissolved in 0.2 ml of 10 mM unbuffered Tris. Quantification of sulforhodamine B was done using an automated enzyme-linked immunosorbent assay plate reader (model 450, Bio-Rad) set at a wavelength of 490 nm. The relative plating efficiency of each clone was determined by dividing the absorbance observed at a given drug concentration by the absorbance detected in the same clone in the absence of drug, and is expressed as a percentage. The degree of resistance is calculated by comparing the IC_{50} value of control cells for a particular drug to the IC_{50} value of Pgp-expressing cells.

Drug Transport Assays. For VBL accumulation, drug-sensitive LR73 control cells and *mdr3*-transfected clones expressing individual mutant Pgps were grown to confluency and harvested by trypsin treatment. Cells were resuspended in complete α-MEM and allowed to recover for 1 h at 20°C. After this period, cells were centrifuged (300*g*, 5 min) and resuspended in PBS containing glucose (50 mM) and glutamine (5 mM), at a final cell density of 4×10^6 cells/ml. Transport was initiated by the addition of [^{3}H]VBL (specific activity of 0.11Ci/mmol; final concentration 1 μM), and at predetermined time intervals 0.5-ml aliquots of cell suspension were centrifuged through a 200-μl cushion of silicone oil/mineral oil (4:1, v:v). The walls of the tube were washed with 1 ml of PBS, and the pellet was dissolved in 1 N NaOH for a minimum of 16 h. The solution was neutralized by the addition of an equivalent volume of 1 N HCl, and samples were removed for analysis of ^{3}H content and protein concentration. For ADM accumulation experiments, drug-sensitive LR73 control cells and *mdr3*-transfected clones were harvested by trypsin treatment and seeded in 6-well titer plates (1.2×10^6/well) in complete Dulbecco's minimal essential medium (10% fetal calf serum, glutamine, and antibiotics). Twenty-four hours later, medium was removed and replaced by Dulbecco's minimal essential medium containing 5% fetal calf serum, [^{14}C]ADM (specific activity, 47.3 μCi/μmol; Amersham Pharmacia Biotech), used at a final concentra-

tion of 2 μM (specific activity, 2.4 μCi/μmol) with glucose and glutamine. At different times after initiation of transport (incubations at 37°C), cells were washed twice with ice-cold PBS and removed from the well by trypsin treatment. Cells were washed once with PBS, and cell-associated radioactivity was measured directly by adding to liquid scintillation fluid (CytoScint; Beckman Instruments, Berkeley, CA), followed by vortexing and scintillation counting. A separate aliquot of cells was used for total protein measurement, and the results are expressed as incorporated [^{14}C]ADM/100 μg of protein.

Calcein-AM Transport Assay. Accumulation of Calcein-AM in control LR73 cells and in pCB6*mdr3* transformants was measured as described previously (Essodaigui et al., 1998). Briefly, 1×10^6 cells from VBL^R mass populations expressing individual *mdr3* mutants were resuspended in HPMI medium (120 mM NaCl, 5 mM KCl, 0.4 mM $MgCl_2$, 0.04 mM $CaCl_2$, 10 mM HEPES-Na, pH 7.4, 10 mM $NaHCO_3$, 10 mM glucose, and 5 mM Na_2HPO_4) and incubated in a quartz cuvette with constant agitation. Cells were incubated with Calcein-AM (0.25 μM), and the fluorescence of the intracellular Calcein was continuously monitored for 20 min. After 12 min, the Pgp inhibitor verapamil (VRP; 15 μM) was added to block efflux of Calcein-AM, and thus establish the specificity of the Pgp-mediated reduction in Calcein accumulation in *mdr3* transfectants. Fluorescence was measured at an excitation wavelength of 493 nm and an emission wavelength of 515 nm in a fluorescence spectrophotometer (F-3010, Hitachi Ltd., Tokyo, Japan).

Immunofluorescence. Cells grown on glass coverslips were washed in PBS and then fixed with 4% paraformaldehyde in PBS for 30 min. After three washes in PBS, cells were then permeabilized by treatment with 0.05% NP-40 in PBS with 1% BSA (Fraction V, Roche Molecular Biochemicals, Indianapolis, IN) and 5% normal goat serum (Life Technologies, Inc., Gaithersburg, MD). Coverslips were washed again with PBS and blocked for 1 h at room temperature in PBS containing 1% BSA and 20% normal goat serum. The cells were incubated with the primary antibody (B2037) diluted 1:4000 in blocking solution for 3 h at room temperature, followed by three washes in PBS containing 0.5% BSA and 0.5% Tween 20. Samples were then incubated with secondary antibody for 30 min (Cy3-conjugated goat anti-rabbit IgG, 1:3000, Jackson Immunoresearch, Avondale, PA), followed by three washes in PBS/BSA/Tween 20, and one final wash in PBS. The coverslips were then mounted onto glass slides in ImmuMount (Shandon, Pittsburgh, PA). Immunofluorescence was analyzed with a Zeiss laser scanning confocal microscope using the 63× oil immersion objective and Zeiss LSM software. The same confocal settings were used to analyze all samples.

Purification of Pgp Mutants and Assay for ATPase Activity. The Mdr3F$_{1-11}$ and W208 mutants were expressed in the yeast *Pichia pastoris* after introduction in the plasmid vector pHILD2, according to a procedure we have described previously (Urbatsch et al., 1998). Positive clones were screened initially by their inability to grow on methanol-containing medium, and were confirmed by immunoblotting analysis of membrane fractions with anti-Pgp monoclonal antibody C219. Purification of Mdr3F$_{1-11}$ and W208 was carried out exactly as we have recently described (Lerner-Marmarosh et al., 1999), except that the starting material consisted of 2-liter cultures of methanol-treated *P. pastoris* cells. Detergent extracts, as well as material binding to and eluting from the Ni^{2+}-NTA column were analyzed by SDS-polyacrylamide gel electrophoresis (PAGE) and Coomassie Blue staining to monitor purification and to evaluate yield and homogeneity of final material. The ATPase activity of the mutant Pgp variants was measured by a P_i release method, as we have described previously (Urbatsch et al., 1998).

Results

Construction and Transfection of a Pgp Mutant Devoid of Tryptophans. Tryptophan fluorescence has been used extensively to study dynamic structure function relationships in various enzymes (Zhou and Rosen, 1997), including integral membrane proteins (Wang et al., 1997). Pgp has a total of 11 tryptophans, with 3 in the membrane-spanning domains (W132, TM2; W228, TM4; W311, TM5), 2 in short extracellular loops (W208, EC2; W851, EC5), 3 in intracellular loops (W44, IC1; W159, IC2; W799, IC4), and 3 in the NB sites (W694/W704, NBD1; W1104, NBD2) (Fig. 1). Considering this large number of Trp residues, it is unlikely that changes in the local environment of individual Trps during either ATP hydrolysis or drug transport by Pgp will be easily interpretable. We constructed a Pgp mutant in which all tryptophans were replaced by the structurally similar phenylalanine (Phe); this mutant can then be used for reintroducing individual Trp residues in strategic locations. For mutagenesis, two mouse *mdr3* cDNA fragments overlapping the amino and carboxyl halves of the protein were subcloned in the M13 plasmid vector. Individual Trp were mutagenized sequentially to Phe using single stranded DNA template, the oligonucleotide primers listed in Table 1, and a commercial mutagenesis system. The full-length Trp-less *mdr3* cDNA (*mdr3*F$_{1-11}$) was reconstructed, its nucleotide sequence was verified, and it was then subcloned in the mammalian expression vector pCB6 (see *Materials and Methods*) for expression in cultured cells. To assess biological activity of the *mdr3*F$_{1-11}$ mutant, drug-sensitive LR73 CHO cells were transfected with pCB6*mdr3*F$_{1-11}$ and mass populations of G418^R colonies were harvested 8 days later. These were then plated in dishes containing increasing concentrations of VBL (25, 50, and 100 ng/ml). At the higher VBL doses (50 and 100 ng/ml), drug-resistant colonies only appeared in cells transfected with wild-type *mdr3*, whereas no colonies formed in the pCB6*mdr3*F$_{1-11}$ group. On the other hand, several VBL^R colonies could be isolated from mass populations of pCB6*mdr3*F$_{1-11}$ transfectants in the lower dose of VBL (25 ng/ml). In additional experiments, several of the pCB6*mdr3*F$_{1-11}$ VBL^R clones selected at 25 ng/ml, were picked and expanded in culture and selected for increasing levels of resistance by subsequent passage in medium containing 50 and 100 ng/ml VBL.

Functional Analysis of *mdr3*F$_{1-11}$-Transfected Clones. As a first step for functional analysis of *mdr3*F$_{1-11}$ transfectants, several independent clones isolated in VBL25 and further expanded in VBL100 were expanded in culture and crude membrane fractions were prepared. These membrane fractions were then analyzed by SDS-PAGE and immunoblotting for the presence of the mutant *mdr3*F$_{1-11}$ Pgp. An analysis of three such pairs of clones (clones 3, 4, and 5) is shown in Fig. 2. In these analyses, two anti-Pgp antibodies were used, the mouse monoclonal C219 that recognizes mouse, hamster, and human Pgp isoforms (Kartner et al., 1985) and the rabbit polyclonal B2037 antiserum (Devault and Gros, 1990), which is species- and isoform-specific for the mouse Mdr3 protein. Membrane fractions from untransfected CHO cells and from cells transfected with the wild-type *mdr3* cDNA and selected in VBL25 and VBL100 were used as negative and positive controls in these experiments. Clones 3 and 4 express a 150- to 160-kDa protein that is detected by the B2037 anti-mouse Mdr3 antibody. This protein is not detected in untransfected CHO LR73 controls and is of identical electrophoretic mobility as that seen in the control cells transfected with WT *mdr3* and selected in the same conditions. This result indicates that the *mdr3*F$_{1-11}$

Pgp is active and confers drug resistance to mammalian cells. Clone 5 is used as an internal control that overexpresses the endogenous hamster Pgp. This hamster Pgp does not react with the anti-mouse Mdr3 B2037 antiserum but instead expresses a C219-reactive protein that is of distinct electrophoretic mobility from the mouse *mdr3*F_{1-11} Pgp, and which is expressed at very low level in the parental CHO cells.

The drug resistance spectrum encoded by the *mdr3*F_{1-11} Pgp mutant was analyzed in cell cytotoxicity assays for the drugs VBL, COL, ACT, and ADM (Fig. 3). The drug concentration required to reduce the plating efficiency of each mass population by 50% (IC_{50}) was measured and is also expressed as a degree of resistance over CHO controls (Table 2). The results of these analyses were very similar for the two independent *mdr3*F_{1-11} Pgp transfectants tested and clearly indicate that the Trp-less mutant encodes a unique drug resistance phenotype distinct from that encoded by either wild-type mouse or hamster Pgps. Indeed, *mdr3*F_{1-11} Pgp transfectants selected in VBL25 showed robust VBL (3×, 4×) and COL (4×, 3×) resistance levels that were similar to those seen in CHO transfectants selected in the same conditions and expressing the hamster Pgp (clone 5). By contrast, the *mdr3*F_{1-11} Pgp mutant conferred very low levels of resistance to ADM (2.4×, 2.1×) and seemed to retain little if any resistance to ACT (1.2×, 0.8×) when compared with wild-type hamster Pgp (ADM, 3×; ACT, 3×). Adaptation of clones 3 and 4 (*mdr3*F_{1-11} Pgp) to growth in VBL100 resulted in a commensurate increase in the level of resistance to this drug (15×, 16×), with final levels of resistance comparable with those seen in CHO transfectants expressing either the wild-type hamster (18×) or mouse Pgp (22×). However, VBL100 selection of clones 3 and 4 caused only a modest increase in resistance to COL (7–9×), ADM (3.3–4×), and in particular ACT (1.8–2×), with final levels of resistance clearly inferior to those measured in cells expressing either wild-type hamster (COL, 26×; ADM, 19×; ACT, 18×) or mouse Pgp (COL, 40×; ADM, 24×; ACT, 50×). These results indicate that the *mdr3*F_{1-11} Pgp does indeed confer drug resistance but with a drug resistance profile quantitatively and qualitatively distinct from its parental counterpart.

Next, we analyzed the kinetics of accumulation of Pgp substrates [^{3}H]VBL (cells in suspension) and [^{14}C]ADM

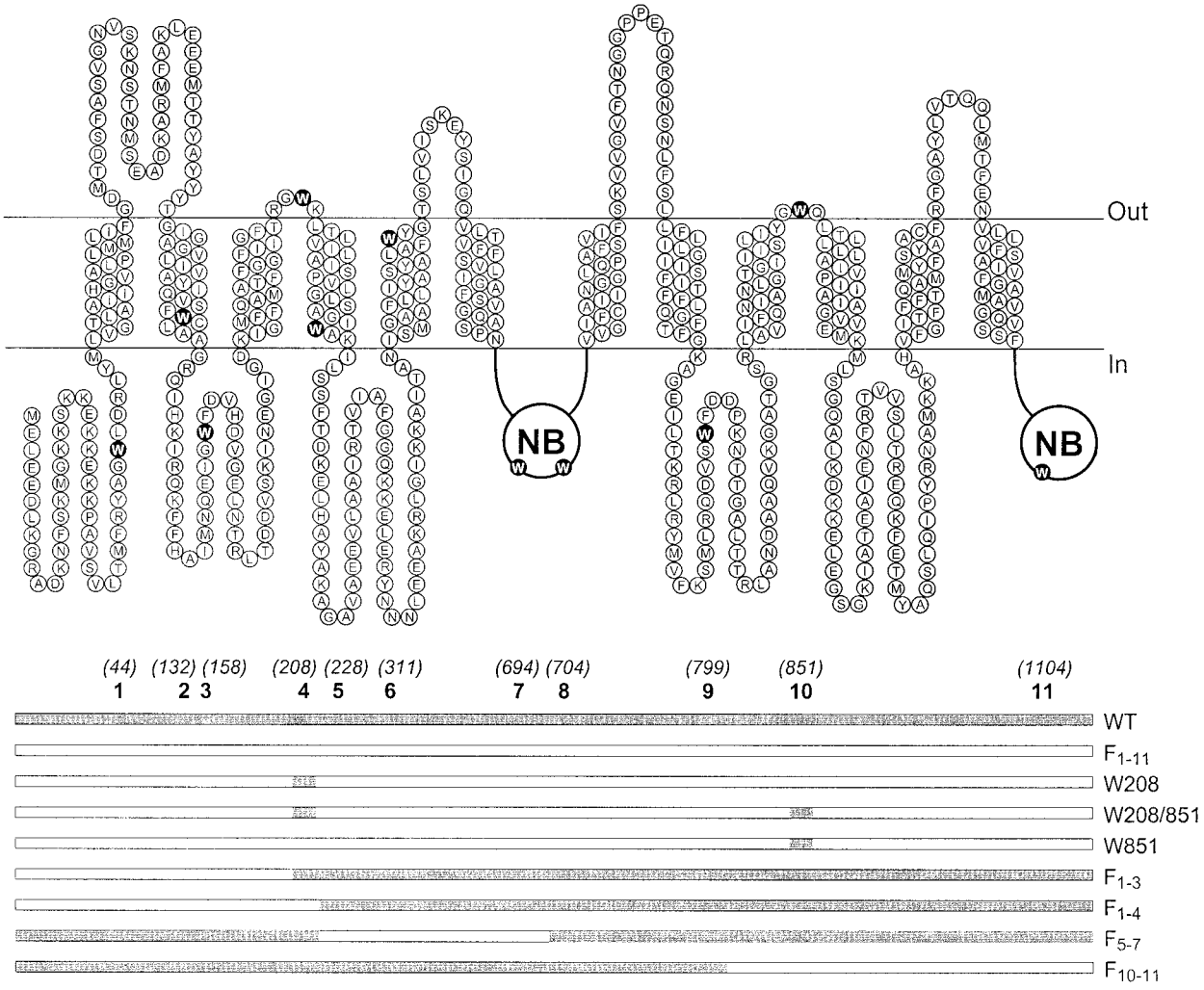

Fig. 1. Secondary structure model of mouse mdr3 and chimeric constructs. Positions of TM domains, extracellular and intracellular loops, and NB domains are shown, and amino acids are represented by the one-letter code. The native tryptophan (Trp) residues are highlighted as black circles with white lettering. Numbering and positions of the 11 Trp are shown below, followed by the construction of the chimeric Mdr3 molecules. Dark bars represent the wild-type Mdr3 backbone, whereas the white portion consists of the Trp-less backbone. The designation of each chimera is shown to the right.

(monolayer cultures) in *mdr3*$F_{1–11}$ Pgp (clones 3, 4), wild-type mouse Mdr3 (WTmdr3), or wild-type hamster Pgp (clone 5) transfectants (Fig. 4, A and B). The *mdr3*$F_{1–11}$ Pgp transfectants can significantly reduce the accumulation of both drugs over a 30- or 180-min assay when compared with nontransfected cells. In general, cells expressing the *mdr3*$F_{1–11}$ Pgp mutant reduced drug accumulation to a level intermediate between that seen in nontransfected controls and that of transfectants expressing either wild-type mouse or hamster Pgps. This was most easily observed when [^{3}H]VBL was used as a substrate and was most obvious for clones selected in VBL25 (low level resistance). We also analyzed the accumulation of another Pgp substrate, Calcein-AM, in these same cell populations (Homolya et al., 1993). Calcein-AM is a nonfluorescent molecule, but once inside the cell, cytoplasmic esterases cleave the acetoxymethyl group and the resulting Calcein molecule becomes fluorescent. In this assay, cells in suspension were incubated in the presence of Calcein-AM and constant monitoring of fluorescence was measured over 12 min. At this point, the Pgp inhibitor VRP was added to the cuvette to block Pgp transport, and fluorescence was further monitored for 8 min (Fig. 4C). In nontransfected CHO cells, we observe a steady rate of accumulation of the fluorescent Calcein molecule inside the cell, and the rate at which fluorescence increases is unaffected when VRP is added. In CHO transfectants, the expression of the *mdr3*$F_{1–11}$ Pgp mutant caused a significant reduction in intracellular accumulation of Calcein-AM over that measured in untransfected CHO controls, during the first 12 min of the assay (early part of the trace). This reduction was not as pronounced as that seen for cells expressing either wild-type mouse (WTmdr3) or hamster Pgp (clone 5), but it was also abrogated by the Pgp inhibitor VRP (arrow on graph). Overall, these results show that the *mdr3*$F_{1–11}$ Pgp mutant retains biological activity, although at a reduced level when compared with wild-type Pgp. This indicates that tryptophan residues are not essential for Pgp function, although their systematic substitution to phenylalanine causes a partial loss of function.

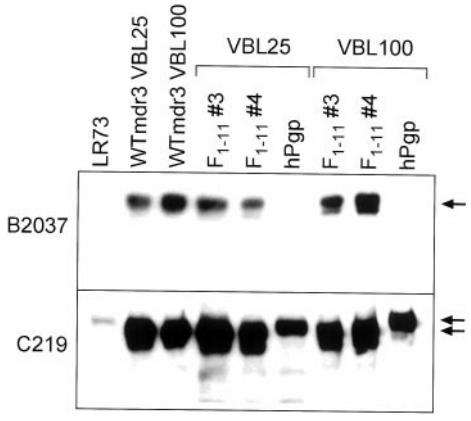

Fig. 2. Immunoblotting of mouse mdr3 mutants. Control drug-sensitive LR73 cells and mass populations of cell clones expressing either wild-type mouse or selected $F_{1–11}$ mutants were passaged in medium containing VBL at 25 ng/ml (VBL25) or at 100 ng/ml (VBL100). Crude membrane fractions were isolated from mass populations of transfected cells. Proteins (10 μg/lane) were resolved on 7.5% SDS-PAGE and analyzed by immunoblotting with either the isoform-specific anti-Mdr3 polyclonal antibody B2037 or the anti-Pgp monoclonal antibody C219. The position of the mouse Pgp is indicated by the single arrow in the top panel. Positions of the hamster and mouse Pgp are shown by the upper and lower arrows, respectively, in the bottom panel.

Characterization of Mdr3 Chimeras and Single Tryptophan Mutants in Mammalian Cells. In the next series of experiments, we wished to determine whether the partial loss of function observed in the *mdr3*$F_{1–11}$ Pgp mutant was associated with the loss of a specific, particularly important tryptophan residue or the result of an additive effect of several tryptophan replacements. For this, we constructed a series of chimeric Mdr3 molecules in which portions of the wild-type protein were inserted in the backbone of the *mdr3*$F_{1–11}$ Pgp mutant to reintroduce different sets of tryptophans. In addition, we reintroduced single tryptophans at positions 208 (W208) and 851 (W851) and at both positions (W208/851) (schematic representation in Fig. 1). The chimeras were cloned into the mammalian expression vector pCB6 and transfected into LR73 CHO cells to assess biological activity. Stable transfectants were selected in G418, and mass populations of $G418^R$ colonies were further selected in two different concentrations of VBL (25 and 50 ng/ml). At VBL25, drug-resistant colonies emerged within 2 weeks of selection for cells transfected with either wild-type *mdr3* or with *mdr3* mutants W208, W851, and W208/851 and chimeras $F_{1–3}$, $F_{1–4}$, $F_{5–7}$, and $F_{10–11}$. Cells transfected with pCB6 alone yielded no drug-resistant colonies in VBL-containing medium.

Expression of the chimeric and mutant Mdr3 proteins in CHO cells was analyzed by Western blotting. Crude membrane fractions from control drug-sensitive cells and cells expressing wild-type and mutant Pgps were separated on 7.5% SDS-PAGE and analyzed using the anti-Pgp antibody C219 (Fig. 5A). A specific immunoreactive band of approximately 140 kDa was seen in all VBL^R *mdr3* transfectants, and this band was absent in control nontransfected CHO cells. Although not identical, the expression levels of the various mutants were found to be similar. An immunoreactive band of 110 kDa could also be seen in all the VBL^R *mdr3* transfectants, in particular in mutants W208/851 and W851. This faster migrating species has been previously suggested to correspond to immature underglycosylated forms of Pgp. The possible functional relevance of this 110-kDa species is unclear, but no correlation between amount of this species and drug resistance phenotype was noted in the various mutants studied. Immunoblotting of the same membrane with the isoform-specific anti-mouse Mdr3 antibody K2037 (Fig. 5A) also confirmed that the immunoreactive band of 140 kDa from the various *mdr3* transfectants corresponds to mouse Mdr3 and is not hamster Pgp overexpressed in clone 5 (hPgP). This indicates that the different Mdr3 chimeras and mutants are all capable of conferring resistance to VBL.

The drug resistance profiles exhibited by the various chimeras and mutants were determined for ACT, VBL, COL, and ADM (Table 3, IC_{50} and fold resistance). Chimeras $F_{1–3}$, $F_{1–4}$, $F_{5–7}$, and $F_{10–11}$ all conferred a higher level of resistance to the four drugs [ACT (10–47×), VBL (24–59×), COL (10–21×), and ADM (3–15×)] compared with *mdr3*$F_{1–11}$ Pgp. On the other hand, the reduced overall activity and altered substrate specificity of *mdr3*$F_{1–11}$ (reduced resistance to ACT and COL, robust resistance to VBL) was recapitulated in *mdr3* mutants bearing single tryptophans at positions 208 (W208), 851 (W851), or at both (W208/851). Finally, all mutants and chimeras, with the exception of $F_{10–11}$, showed

severely impaired resistance to ADM, with an almost 10-fold reduction in IC_{50} value, when compared with our wild-type *mdr3* transfectants. This raised the possibility that a targeting defect mislocalizing the protein intracellularly may account for this more severe selective loss of ADM resistance.

We performed confocal microscopy on permeabilized cells expressing wild-type Mdr3 and a subset of cells expressing the chimeras, which included $F_{1–11}$, W208, W208/851, W851, and $F_{10–11}$. As shown in Fig. 6, we observed that the staining pattern seen in wild-type Mdr3-expressing cells was identical

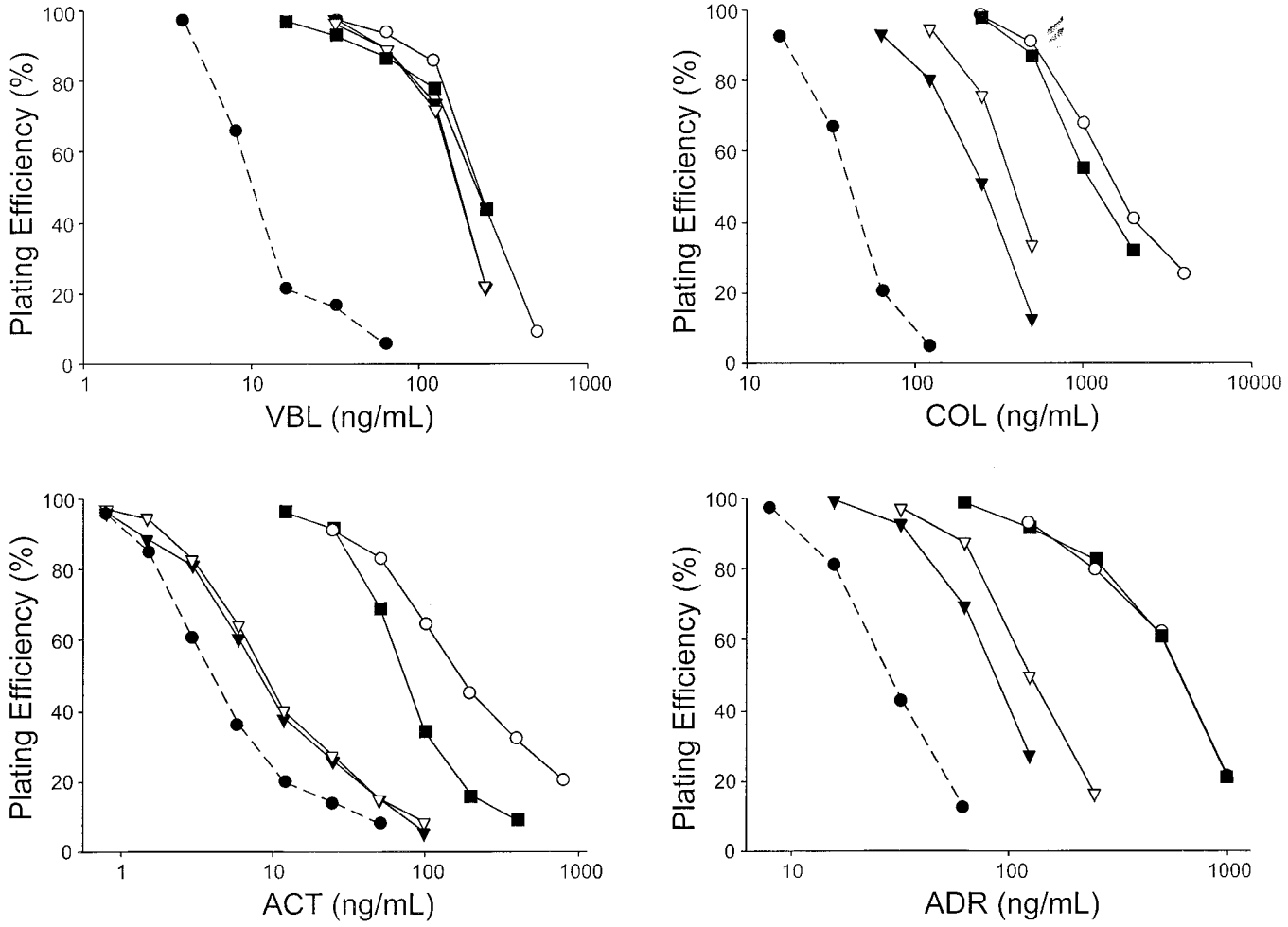

Fig. 3. Drug survival characteristics of transfected LR73 cells expressing wild-type mouse or hamster Pgp or $F_{1–11}$ mutants. Control drug-sensitive LR73 cells (●) and mass populations of cell clones expressing either wild-type mouse (○) or hamster (■) Pgp or selected $F_{1–11}$ mutants (clone 3, ▼; clone 4, ▽) were plated in increasing concentrations of either VBL, COL, ACT, or ADM and further incubated for 72 h. Drug cytotoxicity was measured using a sulforhodamine B staining procedure (*Materials and Methods*). The relative plating efficiency of each cell population was calculated by dividing the absorbance measured at a given drug concentration by the value obtained for the same clone in the absence of drug and was expressed as a percentage. Each point represents the average of three independent experiments performed in duplicate wells.

TABLE 2

Drug survival characteristics of transfected CHO cell clones stably expressing wild-type mouse or hamster Pgp or the selected $F_{1–11}$ mutant

	ACT	VBL	COL	ADM
CHO	5 ± 1 (1×)	17 ± 5[a] (1×)	40 ± 1 (1×)[b]	31 ± 2 (1×)
VBL25				
WTmdr3[c]	250 ± 29 (50×)	378 ± 71 (22×)	1600 ± 55 (40×)	750 ± 150 (24×)
$F_{1–11\ (\#3)}$	6 ± 1 (1.2×)	50 ± 20 (3×)	160 ± 50 (4×)	75 ± 26 (2.4×)
$F_{1–11}$ (#4)	4 ± 1 (0.8×)	65 ± 5 (4×)	108 ± 8 (3×)	66 ± 14 (2.1×)
hPgp	15 ± 8 (3×)	38 ± 17 (2×)	160 ± 10 (4×)	95 ± 5 (3×)
VBL100				
$F_{1–11}$ (#3)	10 ± 1 (2×)	250 ± 50 (15×)	288 ± 35 (7×)	103 ± 18 (3.3×)
$F_{1–11}$ (#4)	9 ± 1 (1.8×)	278 ± 61 (16×)	352 ± 19 (9×)	125 ± 5 (4.0×)
hPgp	89 ± 6 (18×)	308 ± 39 (18×)	1040 ± 24 (26×)	580 ± 20 (19×)

[a] The drug survival of LR73 drug-sensitive cells and multidrug-resistant clones transfected with either wild-type *mdr3* (WT) or mutant genes is expressed as the IC_{50} or the dose necessary to reduce the plating efficiency of the control and transfected cells by 50%. The IC_{50} value is expressed in ng/ml and is an average (±S.E.) of three independent experiments performed in duplicate.

[b] The resistance index is calculated by comparing the IC_{50} value of individual transfectants to that of control LR73 cells and is shown above in parentheses.

[c] Selected in VBL100 ng/ml.

with the cells expressing the chimeric Mdr3 proteins, indicating that the different Mdr3 chimeras are all present at the plasma membrane.

The ability of the Mdr3 chimeras and single tryptophan mutants to transport Calcein-AM also was examined. In all the VBL^R clones expressing wild-type Mdr3 and Mdr3 mutants, a significantly decreased accumulation of Calcein in the cytoplasm was observed (Fig. 5B). Furthermore, addition of the Pgp inhibitor VRP resulted in increased accumulation and fluorescence of Calcein at a rate similar to that in nontransfected CHO cells. The levels of Calcein-AM transport in wild-type and mutant Mdr3-expressing cells was similar in all cases, as was the degree of inhibition by VRP. These results verify that all Mdr3 chimeras and mutants are competent for transport and retain susceptibility to inhibition by VRP. Although we did not measure true efflux rates, these results and those shown in Fig. 4 suggest that it is the drug export function of Pgp that is impaired in these mutants. These results suggest that no single tryptophan residue is responsible for the partial loss of function and unique phenotype of the *mdr3*F_{1-11} Pgp mutant.

ATPase Activity of the Mdr3F_{1-11} and W208 Mutants. The Mdr3F_{1-11} and W208 mutants were expressed in the yeast *P. Pastoris* and purified (Fig. 7A) according to a protocol recently described (Lerner-Marmarosh et al., 1999) and based on dodecyl maltoside extraction of Pgp from microsome-rich fractions, followed by affinity chromatography on Ni^{2+}-NTA resin, and final purification by ion exchange chromatography on DE-52 resin (see *Materials and Methods*). Results from purification experiments (Fig. 7A) show a significant degree of enrichment of wild-type and mutant protein in the imidazole (200 mM) eluate of the Ni^{2+}-NTA resin and show excellent purification of the Mdr3F_{1-11} (1 μg), W208, (2 μg), and WT Mdr3 (5 μg) on subsequent DE-52 chromatography. The purified proteins were reconstituted in the presence of dithiothreitol and *Escherichia coli* lipids and then assayed for ATPase activity. As shown in Fig. 7B, wild-type Pgp and the Mdr3F_{1-11} and Mdr3W208 mutants displayed low and variable levels of basal ATPase activity; however, ATP hydrolysis by the wild-type protein was greatly enhanced with the addition of 50 μM VRP in agreement with previously published data (Lerner-Marmarosh et al., 1999). In contrast, mutants Mdr3F_{1-11} and W208 also displayed VRP-induced ATPase activity, although the level of stimulation was smaller than that seen in wild-type Mdr3, with 2.9× and 3.4×, respectively, observed. These results show that removal of all tryptophan residues in the Mdr3F_{1-11} mutant results in a significant reduction of the drug-inducible ATPase activity of the protein, which correlates with the partial loss of activity of this protein noted in drug resistance and drug transport assays.

Discussion

Most of the structural information on Pgp has been gathered from computer-assisted analysis of the predicted amino acid sequence of the protein (hydropathy) (Gros et al., 1986), classical biochemical (mapping of photolabeled proteolytic fragments) (Yoshimura et al., 1989), and immunological analyses (epitope mapping) (Kast et al., 1996) as well as low resolution structure (2.5 nm) by electron microscopy and single particle image analysis (Rosenberg et al., 1997). Additional information has been obtained from the study of single cysteine Pgp mutants constructed on a cysteine-less background, which can be modified by cysteine-reactive sulfhydryl reagents. A combination of membrane permeant and impermeant maleimide reagents has been used in various single cysteine mutants to study the topology of individual TM domains of Pgp (Loo and Clarke, 1995b), monitor the activity of individual NB sites (Loo and Clarke, 1995a), and map individual residues contributing to substrate binding (Loo and Clarke, 1996, 1997b). This mutant has also been

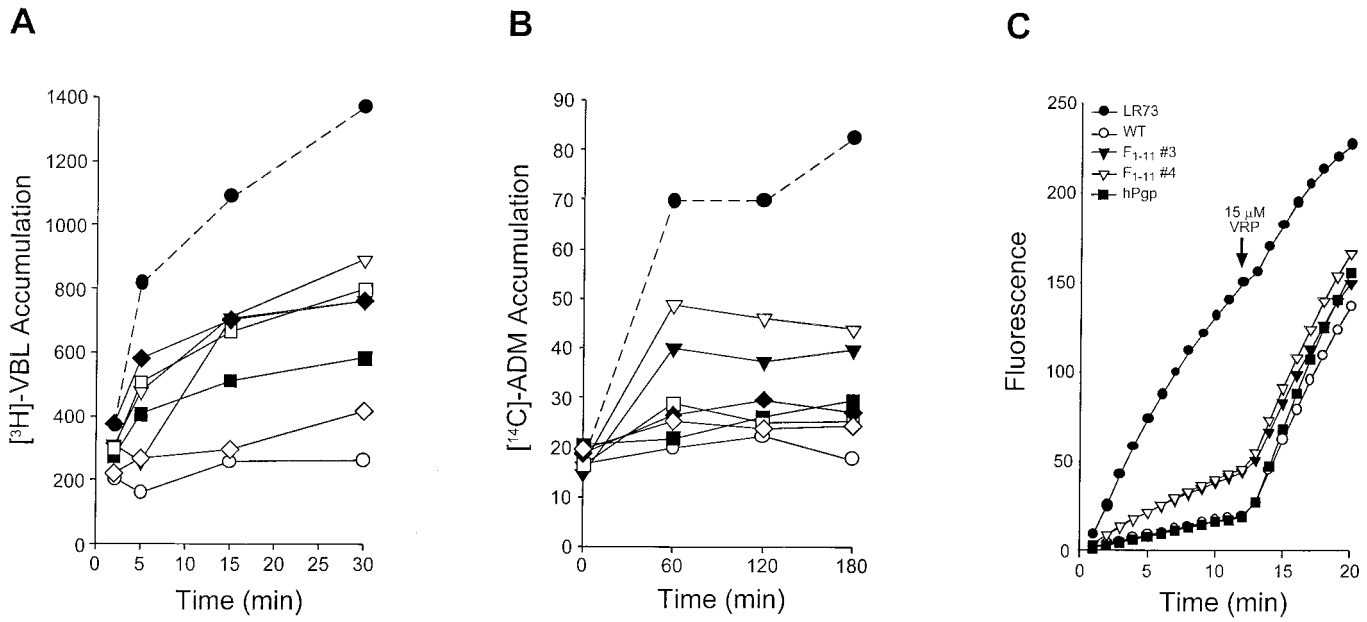

Fig. 4. Functional analysis of transfected LR73 cells expressing wild-type mouse or hamster Pgp or F_{1-11} mutants. Time-dependent accumulation of [^{3}H]VBL (A) and [^{14}C]ADM (B) by mass populations of untransfected LR73 cells (●) and clones expressing wild-type mouse (○) or hamster Pgp (VBL25, ■; VBL100, ◇) or selected F_{1-11} mutants (VBL25: clone 3, ▼; clone 4, ▽; VBL100: clone 3, □; clone 4, ◆). C, time-dependent accumulation of Calcein-AM and measurement of relative fluorescence intensity of free intracellular Calcein.

used in cross-linking experiments to establish proximity relationships between individual TM domains (Loo and Clarke, 1996, 1997a,b). Finally, cysteine mutants cross-linked with fluorescent maleimide derivatives have been used in fluorescence energy transfer experiments with fluorescent lipid molecules and/or drug substrates to detect structural and/or functional interactions between the membrane domains and the NB sites (Liu and Sharom, 1998).

Fluorescence spectroscopy, which takes advantage of either covalently linked fluorescent reporter molecules or the intrinsic fluorescence of tryptophan or tyrosine residues, is an attractive alternative to study such interactions. In these experiments, intrinsic fluorescence of tryptophan residues can be altered qualitatively (emission wavelength) or quantitatively (emission intensity) by changes in the environment of individual tryptophan residues, including quenching by substrate or inhibitor molecules located in close proximity. This method has been used extensively to identify structure/function relationships in soluble as well as integral membrane proteins. Examples are the study of the catalytic cycle of F1-ATPase (Weber et al., 1998), monitoring dynamic changes in the NB site of the bacterial arsenite extrusion pump during ATP hydrolysis (Zhou and Rosen, 1997), and probing the interaction of lactose analogs with individual membrane domains of the lactose permease of *E. coli* (Wang et al., 1997). A major limitation of fluorescence studies using endogenous tryptophan residues is the potential complexity of the signal produced by multiple tryptophans in the protein. This can be alleviated by mutational modification to remove all tryptophans from the protein followed by reintroduction of single tryptophans at strategic positions in this Trp-less backbone.

To this end, we have constructed a mouse Mdr3 Pgp mutant in which all 11 tryptophans have been changed to phenylalanine (*mdr3*F_{1-11}). The *mdr3*F_{1-11} Pgp mutant is expressed in the membrane fraction of transfected cells, confers drug resistance, and is active in drug transport assays using three known Pgp substrates, Calcein-AM, ADM, and VBL. This result indicates that none of the 11 endogenous Trp residues of Pgp are essential for function. Additional characterization of the *mdr3*F_{1-11} mutant indicates a decrease in overall activity when compared with wild-type Pgp, as well as a deviation in the drug resistance profile conveyed in CHO cells when compared with either wild-type mouse or hamster Pgp. The unique drug resistance phenotype of the F_{1-11} mutant is unlikely to be caused by the selection procedure used, as it was seen in independent cell clones expressing this protein. In addition, we have shown previously that selection of transfected cell clones in low concentrations of VBL has no effect on the drug resistance profile conveyed by wild-type or

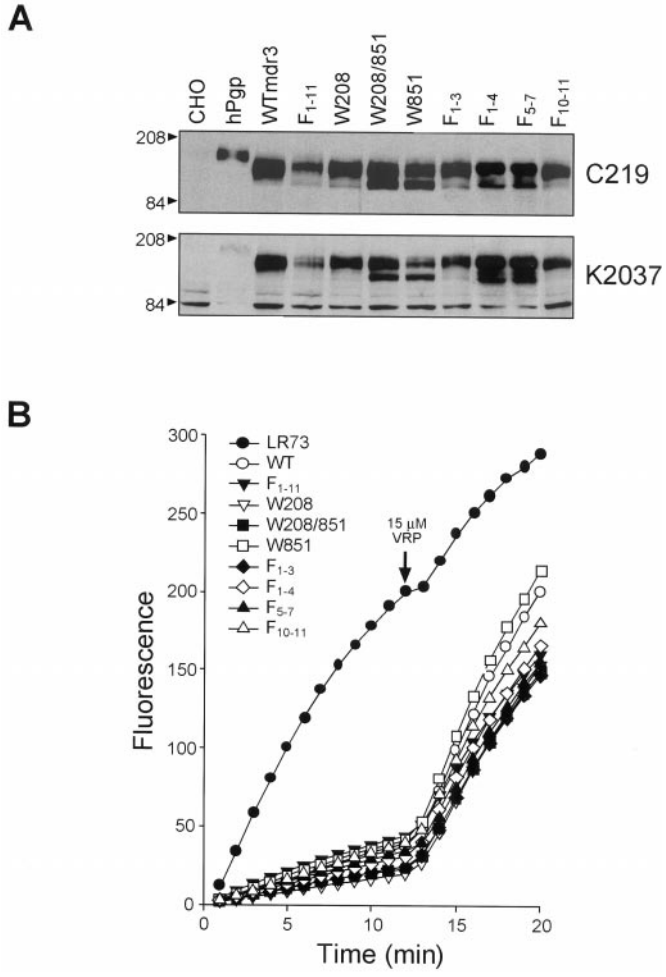

Fig. 5. Functional analysis of chimeric mdr3 mutants. A, immunoblotting of control drug-sensitive LR73 cells and mass populations of cell clones expressing wild-type hamster (hPgp) or mouse (WTmdr3) Pgp or various chimeric Mdr3 proteins. Crude membrane fractions were isolated, and 10 μg of protein was resolved on 7.5% SDS-PAGE and analyzed by immunoblotting with either the anti-Pgp monoclonal antibody C219 or the isoform-specific anti-Mdr3 polyclonal antibody K2037. B, time-dependent accumulation of Calcein-AM and measurement of relative fluorescence intensity of free intracellular Calcein by mass populations of cell clones expressing wild-type mouse Mdr3 or chimeric Mdr3 proteins.

TABLE 3
Drug survival characteristics of hamster cell clones stably expressing wild-type and mutant *mdr3* genes

	ACT	VBL	COL	ADM
LR73	5 ± 1[a] (1×)	10 ± 1 (1×)[b]	47 ± 3 (1×)	22 ± 1 (1×)
WTmdr3	314 ± 34 (63×)	486 ± 45 (49×)	2560 ± 229 (54×)	680 ± 71 (31×)
F_{1-11}	5 ± 1 (1×)	163 ± 13 (16×)	190 ± 40 (4×)	40 ± 5 (2×)
W208	58 ± 6 (12×)	330 ± 45 (33×)	503 ± 104 (11×)	70 ± 6 (3×)
W208/851	15 ± 3 (3×)	230 ± 10 (23×)	437 ± 26 (9×)	91 ± 7 (4×)
W851	9 ± 2 (2×)	160 ± 10 (16×)	140 ± 60 (3×)	40 ± 2 (2×)
F_{1-3}	50 ± 10 (10×)	365 ± 37 (37×)	483 ± 120 (10×)	57 ± 12 (3×)
F_{1-4}	76 ± 5 (15×)	515 ± 105 (52×)	655 ± 255 (14×)	78 ± 0 (4×)
F_{5-7}	88 ± 8 (18×)	585 ± 35 (59×)	700 ± 250 (15×)	85 ± 4 (4×)
F_{10-11}	235 ± 85 (47×)	235 ± 15 (24×)	1010 ± 143 (21×)	327 ± 12 (15×)

[a] The drug survival of LR73 drug-sensitive cells and multidrug-resistant clones transfected with either wild-type *mdr3* (WT) or mutant genes is expressed as the IC_{50} or the dose necessary to reduce the plating efficiency of the control and transfected cells by 50%. The IC_{50} value is expressed in ng/ml and is an average (±S.E.) of three independent experiments performed in duplicate.
[b] The resistance index is calculated by comparing the IC_{50} value of individual transfectants to that of control LR73 cells and is shown above in parentheses.

mutant Pgp variants (Beaudet and Gros, 1995). Likewise, we noted that the *mdr3*F_{1-11} mutant loses the ability to confer resistance to the fungicide FK506 in yeast and fails to complement a null *ste6* yeast mutant (data not shown), known characteristics of the wild-type mouse Mdr3 protein (Raymond et al., 1992, 1994). Studies of single and double tryptophan mutants and chimeric proteins constructed between wild-type Pgp and *mdr3*F_{1-11} indicate that the partial loss of function of *mdr3*F_{1-11} is not caused by the loss of any uniquely important Trp residues but is, rather, the result of a cumulative loss of several Trp residues. Studies of the VRP-stimulated ATPase activity of the mdr3F_{1-11} and W208 mutants indicate that partial loss of drug resistance in these mutants is concomitant to a partial loss of ATPase activity (F_{1-11}, 2.9× stimulation; W208, 3.4× stimulation). These results support a loss of catalytic activity, as opposed to mistargeting of the mutant enzymes to explain the partial loss of Pgp function observed. Characterization of the drug resistance profiles conveyed by the *mdr3*F_{1-11} mutant, and by the additional mutants in which the majority of tryptophans had been substituted by phenylalanine revealed an intriguing low level resistance of all the mutants (with the exception of F_{10-11}) toward the drug ADM. This finding was surprising, because 1) some of the mutants show near wild type levels of resistance to other drugs and 2) drug transport assays in the *mdr3*F_{1-11} mutant for the drug ADM showed a fairly robust transport activity of the mutant toward this drug. The potential causes of this unique phenotype remain unclear. One possibility is that the elimination of one or more tryptophans in Pgp affects protein maturation and targeting. Although this may have little effect on the ability of the corresponding transfectants to prevent drug accumulation in a short-term transport assay, it may nevertheless result in a small increase in steady-state accumulation of ADM only detectable in a longer term cell cytotoxicity assay. This was investigated using confocal microscopy of permeabilized CHO cells expressing the various *mdr3* mutants. There appears to be no major defect in targeting of the protein to the plasma membrane, because all the mutants show a ring-like staining indicative of plasma membrane expression similar to the wild-type *mdr3* protein (Fig. 6).

The *mdr3*F_{1-11} mutant constructed here can now be used as a molecular backbone to introduce individual tryptophans at strategic locations in the protein to monitor dynamic changes in local environments as a function of transport or catalytic activity of the protein. Of particular interest are the two single tryptophan mutants already available (W208 and W851) that map, in short extracellular loops of Mdr3 proximal to membrane-spanning domains, regions that have been shown to be involved in drug binding. The effect of different

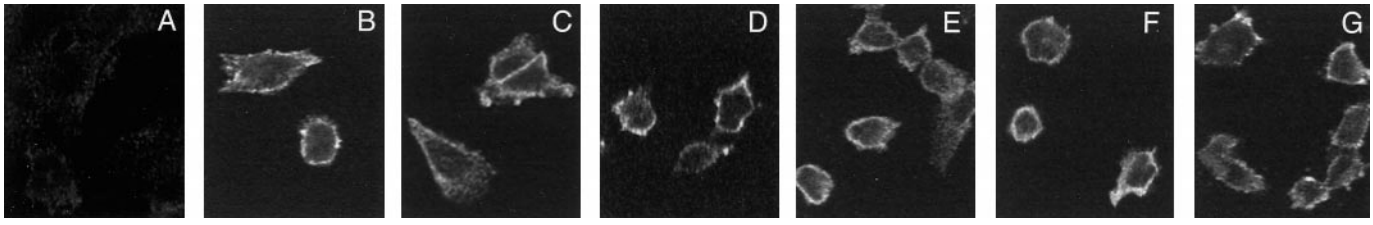

Fig. 6. Immunofluorescence of chimeric mdr3 mutants. Untransfected cells (A) or cells expressing (B) wild-type *mdr3*, (C) *mdr3*F_{1-11}, (D) *mdr3*W208, (E) *mdr3*W208/851, (F) *mdr3*W851, or (G) *mdr3*F_{10-11} were analyzed using immunofluorescence. Cells were fixed, permeabilized, and blocked as described under *Materials and Methods* followed by exposure to the rabbit anti-mouse Pgp antiserum B2037, then by incubation with a second goat anti-rabbit antibody conjugated to Cy3. Cells were visualized and photographed using a confocal microscope as described previously.

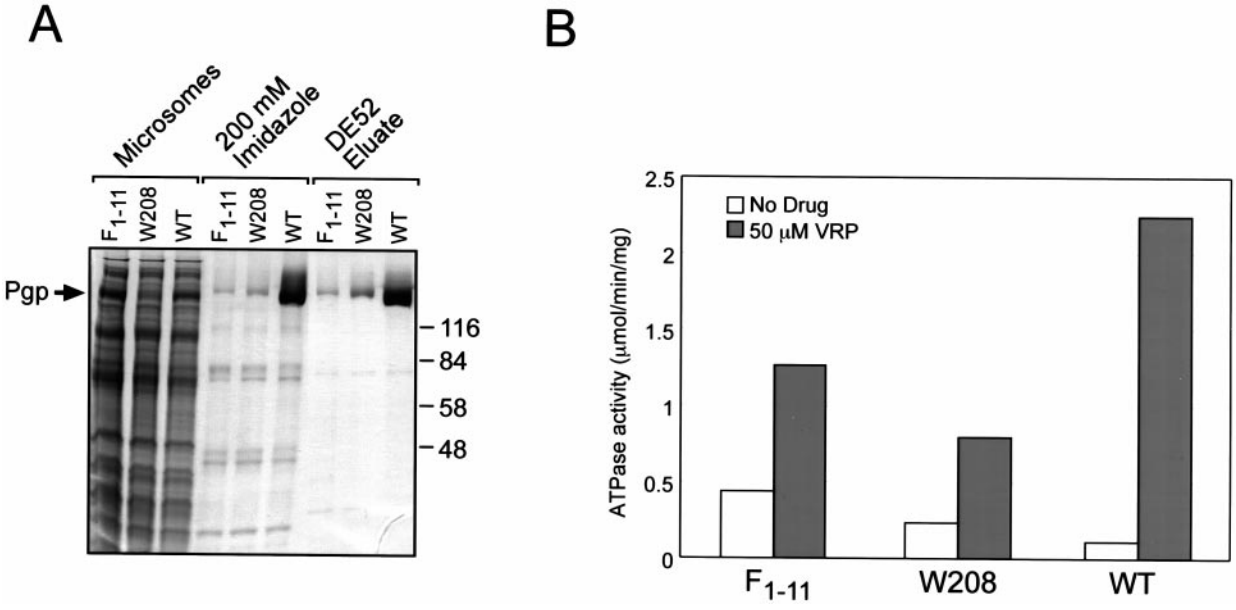

Fig. 7. Purification of Pgp mutants and assay of ATPase activity. A, Coomassie Blue-stained 7.5% SDS-containing polyacrylamide gel of wild-type Mdr3, Mdr3F_{1-11}, and W208 at different purification steps, including microsomal membranes (15 μg), 200 mM imidazole eluate from an Ni^{2+}-NTA column (5 μg), and flow-through from DE52 column. B, ATPase activity of wild-type Pgp and Mdr3F_{1-11} and W208 mutants purified from *P. Pastoris*. Purified protein fractions were assayed for ATPase activity in the presence (gray bars) or absence (white bars) of 50 μM VRP.

Pgp substrates and inhibitors on intrinsic fluorescence of these two tryptophans should help investigators understand the nature and complexity of the drug binding site(s) of Pgp. Likewise, the insertion of single tryptophans in either NB site should make possible additional probes of the catalytic cycle of the Pgp ATPase, including understanding dynamic changes at the NB sites associated with drug binding at the TM regions.

References

Azzaria M, Schurr E and Gros P (1989) Discrete mutations introduced in the predicted nucleotide-binding sites of the mdr1 gene abolish its ability to confer multidrug resistance. *Mol Cell Biol* **9:**5289–5297.

Beaudet L and Gros P (1995) Functional dissection of P-glycoprotein nucleotide-binding domains in chimeric and mutant proteins: Modulation of drug resistance profiles. *J Biol Chem* **270:**17159–17170.

Brewer CB (1994) Cytomegalovirus plasmid vectors for permanent lines of polarized epithelial cells. *Methods Cell Biol* **43:**233–245.

Devault A and Gros P (1990) Two members of the mouse mdr gene family confer multidrug resistance with overlapping but distinct drug specificities. *Mol Cell Biol* **10:**1652–1663.

Devine SE, Ling V and Melera PW (1992) Amino acid substitutions in the sixth transmembrane domain of P-glycoprotein alter multidrug resistance. *Proc Natl Acad Sci USA* **89:**4564–4568.

Essodaigui M, Broxterman HJ and Garnier-Suillerot A (1998) Kinetic analysis of calcein and calcein-acetoxymethylester efflux mediated by the multidrug resistance protein and P-glycoprotein. *Biochemistry* **37:**2243–2250.

Greenberger LM (1993) Major photoaffinity drug labeling sites for iodoaryl azidoprazosin in P-glycoprotein are within, or immediately C-terminal to, transmembrane domains 6 and 12. *J Biol Chem* **268:**11417–11425.

Gros P, Croop J and Housman D (1986) Mammalian multidrug resistance gene: Complete cDNA sequence indicates strong homology to bacterial transport proteins. *Cell* **47:**371–380.

Hafkemeyer P, Dey S, Ambudkar SV, Hrycyna CA, Pastan I and Gottesman MM (1998) Contribution to substrate specificity and transport of nonconserved residues in transmembrane domain 12 of human P-glycoprotein. *Biochemistry* **37:**16400–16409.

Hanna M, Brault M, Kwan T, Kast C and Gros P (1996) Mutagenesis of transmembrane domain 11 of P-glycoprotein by alanine scanning. *Biochemistry* **35:**3625–3635.

Hanna M and Gros P (1996) Cloning and structure: Function analysis of the mouse mdr gene family, in *Multidrug Resistance in Cancer Cells: Molecular, Biochemical, Physiological and Biological Aspects* (Gupta S and Tsuruo T eds) pp 5–28, John Wiley and Sons, New York.

Homolya L, Hollo Z, Germann UA, Pastan I, Gottesman MM and Sarkadi B (1993) Fluorescent cellular indicators are extruded by the multidrug resistance protein. *J Biol Chem* **268:**21493–21496.

Kartner N, Evernden-Porelle D, Bradley G and Ling V (1985) Detection of P-glycoprotein in multidrug-resistant cell lines by monoclonal antibodies. *Nature (Lond)* **316:**820–823.

Kast C, Canfield V, Levenson R and Gros P (1995) Membrane topology of P-glycoprotein as determined by epitope insertion: Transmembrane organization of the N-terminal domain of mdr3. *Biochemistry* **34:**4402–4411.

Kast C, Canfield V, Levenson R and Gros P (1996) Transmembrane organization of mouse P-glycoprotein determined by epitope insertion and immunofluorescence. *J Biol Chem* **271:**9240–9248.

Lerner-Marmarosh N, Gimi K, Urbatsch IL, Gros P and Senior AE (1999) Large scale purification of detergent-soluble P-glycoprotein from *Pichia pastoris* cells and characterization of nucleotide binding properties of wild-type, Walker A, and Walker B mutant proteins. *J Biol Chem* **274:**34711–34718.

Ling V (1997) Multidrug resistance: Molecular mechanisms and clinical relevance. *Cancer Chemother Pharmacol* **40:**S3–S8.

Liu R and Sharom FJ (1996) Site-directed fluorescence labeling of P-glycoprotein on cysteine residues in the nucleotide binding domains. *Biochemistry* **35:**11865–11873.

Liu R and Sharom FJ (1998) Proximity of the nucleotide binding domains of the P-glycoprotein multidrug transporter to the membrane surface: A resonance energy transfer study. *Biochemistry* **37:**6503–6512.

Loo TW and Clarke DM (1994) Mutations to amino acids located in predicted transmembrane segment 6 (TM6) modulate the activity and substrate specificity of human P-glycoprotein. *Biochemistry* **33:**14049–14057.

Loo TW and Clarke DM (1995a) Covalent modification of human P-glycoprotein mutants containing a single cysteine in either nucleotide-binding fold abolishes drug-stimulated ATPase activity. *J Biol Chem* **270:**22957–22961.

Loo TW and Clarke DM (1995b) Membrane topology of a cysteine-less mutant of human P-glycoprotein. *J Biol Chem* **270:**843–848.

Loo TW and Clarke DM (1996) Inhibition of oxidative cross-linking between engineered cysteine residues at positions 332 in predicted transmembrane segments (TM) 6 and 975 in predicted TM12 of human P-glycoprotein by drug substrates. *J Biol Chem* **271:**27482–27487.

Loo TW and Clarke DM (1997a) Drug-stimulated ATPase activity of human P-glycoprotein requires movement between transmembrane segments 6 and 12. *J Biol Chem* **272:**20986–20989.

Loo TW and Clarke DM (1997b) Identification of residues in the drug-binding site of human P-glycoprotein using a thiol-reactive substrate. *J Biol Chem* **272:**31945–31948.

Raymond M, Gros P, Whiteway M and Thomas DY (1992) Functional complementation of yeast ste6 by a mammalian multidrug resistance mdr gene. *Science (Wash DC)* **256:**232–234.

Raymond M, Ruetz S, Thomas DY and Gros P (1994) Functional expression of P-glycoprotein in *Saccharomyces cerevisiae* confers cellular resistance to the immunosuppressive and antifungal agent FK520. *Mol Cell Biol* **14:**277–286.

Rosenberg MF, Callaghan R, Ford RC and Higgins CF (1997) Structure of the multidrug resistance P-glycoprotein to 2.5 nm resolution determined by electron microscopy and image analysis. *J Biol Chem* **272:**10685–10694.

Ruetz S and Gros P (1994) Phosphatidylcholine translocase: A physiological role for the mdr2 gene. *Cell* **77:**1071–1081.

Schinkel AH, Smit JJ, van Tellingen O, Beijnen JH, Wagenaar E, van Deemter L, Mol CA, van der Valk MA, Robanus-Maandag EC, te Riele HP, Berns AJM and Borst P (1994) Disruption of the mouse mdr1a P-glycoprotein gene leads to a deficiency in the blood-brain barrier and to increased sensitivity to drugs. *Cell* **77:**491–502.

Senior AE (1998) Catalytic mechanism of P-glycoprotein. *Acta Physiol Scand Suppl* **643:**213–218.

Shapiro AB and Ling V (1998) The mechanism of ATP-dependent multidrug transport by P-glycoprotein. *Acta Physiol Scand Suppl* **643:**227–234.

Tang-Wai DF, Brossi A, Arnold LD and Gros P (1993) The nitrogen of the acetamido group of colchicine modulates P-glycoprotein-mediated multidrug resistance. *Biochemistry* **32:**6470–6476.

Urbatsch IL, Beaudet L, Carrier I and Gros P (1998) Mutations in either nucleotide-binding site of P-glycoprotein (Mdr3) prevent vanadate trapping of nucleotide at both sites. *Biochemistry* **37:**4592–4602.

Vanhelvoort A, Smith AJ, Sprong H, Fritzsche I, Schinkel AH, Borst P and Vanmeer G (1996) mdr1 P-glycoprotein is a lipid translocase of broad specificity, while mdr3 P-glycoprotein specifically translocates phosphatidylcholine. *Cell* **87:**507–517.

Vernet T, Dignard D and Thomas DY (1987) A family of yeast expression vectors containing the phage f1 intergenic region. *Gene* **52:**225–233.

Wang Q, Matsushita K, de Foresta B, le Maire M and Kaback HR (1997) Ligand-induced movement of helix X in the lactose permease from *Escherichia coli*: A fluorescence quenching study. *Biochemistry* **36:**14120–14127.

Weber J, Wilke-Mounts S, Hammond ST and Senior AE (1998) Tryptophan substitutions surrounding the nucleotide in catalytic sites of F1-ATPase. *Biochemistry* **37:**12042–12050.

Yoshimura A, Kuwazuru Y, Sumizawa T, Ichikawa M, Ikeda S, Uda T and Akiyama S (1989) Cytoplasmic orientation and two-domain structure of the multidrug transporter, P-glycoprotein, demonstrated with sequence-specific antibodies. *J Biol Chem* **264:**16282–16291.

Zhou T and Rosen BP (1997) Tryptophan fluorescence reports nucleotide-induced conformational changes in a domain of the ArsA ATPase. *J Biol Chem* **272:**19731–19737.

Send reprint requests to: Philippe Gros, Department of Biochemistry, McGill University, 3655 Drummond St., Montreal, Quebec, H3G 1Y6 Canada. E-mail: gros@med.mcgill.ca